Proc. Natl. Acad. Sci. USA
Vol. 92, pp. 9402–9406, September 1995
Biophysics

Identification of the overtone of the Fe–CO stretching mode in heme proteins: A probe of the heme active site

JIANLING WANG, SATOSHI TAKAHASHI, AND DENIS L. ROUSSEAU†

AT&T Bell Laboratories, Murray Hill, NJ 07974

Communicated by Hans Frauenfelder, Los Alamos National Laboratory, Los Alamos, NM, June 2, 1995 (received for review October 18, 1994)

ABSTRACT **Two CO-isotope sensitive lines have been detected in the overtone region of the resonance Raman spectra of CO-bound hemeproteins. One line is assigned as the overtone of the Fe–CO stretching mode and is located in the 1000- to 1070-cm^{-1} region. The other line is found in the 1180- to 1210-cm^{-1} region and is assigned as a combination between a porphyrin mode, ν_7, and the Fe–CO stretching mode. The high intensities of these lines, which in the terminal oxidase class of proteins are of the same order as those of the fundamental stretching mode, indicate that the mechanism of enhancement for modes involving the Fe–CO moiety is different from that for the modes of the porphyrin macrocycle and call for reexamination of Raman theory of porphyrins as applied to axial ligands. The anharmonicity of the electronic potential function was evaluated, revealing that in the terminal oxidases the anharmonicity is greater than in the other heme proteins that were examined, suggesting a distinctive interaction of the bound CO with its distal environment in this family. Furthermore, the anharmonicity correlates with the frequency of the C–O stretching mode, demonstrating that both of these parameters are sensitive to the Fe–CO bond energy. The overtone and combination lines involving the bound CO promise to be additional probes of heme protein structural properties.**

Heme proteins, which function either as oxygen carriers or as catalytic enzymes, have a pocket on the distal side of the heme in which exogenous ligands bind to the iron atom. The function of the heme protein depends critically on the properties of the distal pocket and how its residues interact with the heme-bound exogenous ligands. Studies of CO adducts of heme proteins have been shown to be extremely important probes of the active sites, including the interactions between the CO and the distal residues (1, 2). In addition, CO photodissociation and recombination studies have played an essential role in unraveling the dynamic processes that occur in heme proteins, information which has led to an advanced understanding of the basic physics that forms the foundation of the physiological process of ligand binding (3, 4).

Structural information such as the identity of the proximal ligand, the geometry of the bound CO, and the interactions between the axial ligands and the heme environment has been determined from the vibrational spectra of the fundamental modes involving the CO. However, overtones offer the possibility of yielding additional information concerning the heme pocket and the electronic structure because the behavior of the overtones depends critically on the shape of the ground-state potential function as well as the properties of the excited electronic state. In the overtone region of the Fe–CO stretching mode (ν_{Fe-CO}) two lines have been independently discovered recently (5, 6). We assign one as the overtone (ν_{over}) of the Fe–CO stretching mode and the second as a combination (ν_{comb}) of the Fe–CO stretching mode with a mode of the porphyrin macrocycle (ν_7). These modes are probes of the active site of heme proteins.

MATERIALS AND METHODS

Cytochrome *c* oxidase and quinol oxidase (cytochrome bo_3) were isolated and purified in our laboratories from bovine heart and *Escherichia coli*, respectively, by reported procedures (7, 8). Cytochrome *c* peroxidase (*Cc*P) was extracted from bakers' yeast and crystallized by a modified procedure (9). Myoglobin (horse skeletal) was purchased from Sigma and used without further purification. Gases of natural and isotopic CO were obtained from Matheson and ICON Services (Summit, NJ), respectively.

The Raman data were collected as reported previously (10). Typically, CO-bound samples (130 μl, 20–80 μM) were prepared, in a sealed spinning cell, by exposing the reduced protein to the natural abundance or isotopically enriched CO gas. The excitation wavelength of 413.1 nm (power, 0.1–3 mW) was used in most cases to optimize the intensities of overtone and combination lines. The frequencies of the Raman lines were calibrated against an indene standard or laser fluorescence lines. Spectra shown here were unsmoothed but baseline-corrected, which does not lead to any significant shifts in the peak frequencies. The parameters for the anharmonicity were evaluated by subtraction of the average of the two isotope-labeled lines of ν_{over}, from twice the average of the two isotope-labeled lines ($^{12}C^{16}O$ and $^{13}C^{18}O$) of the ν_{Fe-CO} fundamental mode. The current data are the average of two sets of independent readings. The intensities of the ν_{Fe-CO} fundamental, overtone (I_{over}) and combination (I_{comb}) modes were estimated by measuring the areas of corresponding peaks in the $^{12}C^{16}O$–$^{13}C^{18}O$ spectra.

RESULTS AND DISCUSSION

Line Assignments. The resonance Raman spectra of cytochrome *c* oxidase from 350 to 2000 cm^{-1} coordinated by $^{12}C^{16}O$ (spectrum a) and $^{13}C^{18}O$ (spectrum b) are shown in Fig. 1. The lines at 519, 577, and 1963 cm^{-1} in the spectrum of the $^{12}C^{16}O$ adduct are assigned as the Fe–CO stretching (ν_{Fe-CO}), the Fe–C–O bending (δ_{Fe-C-O}), and the C–O stretching (ν_{C-O}) modes, respectively, in accord with previous assignments (11, 12). These three modes shift to lower frequency in the $^{13}C^{18}O$ adduct, as expected for the heavier isotopes and as readily seen in the difference spectrum reported in the spectrum c of Fig. 1. Two new lines at 1026 and 1201 cm^{-1} for the $^{12}C^{16}O$ adduct are also present in the difference spectrum. Fig. 2 depicts the spectra of several other heme proteins, and the data are summarized in Table 1. The modes are detected in a variety of proteins, ranging from those in which the heme is coordinated by a neutral imidazole, such as in the hemoglobins (spectra d and f) and myoglobin (spectrum g), to that in which the heme

The publication costs of this article were defrayed in part by page charge payment. This article must therefore be hereby marked "*advertisement*" in accordance with 18 U.S.C. §1734 solely to indicate this fact.

Abbreviations: *Cc*P, cytochrome *c* peroxidase; I_{over}, intensity of the overtone mode; I_{comb}, intensity of the combination mode.

†To whom reprint requests should be addressed.

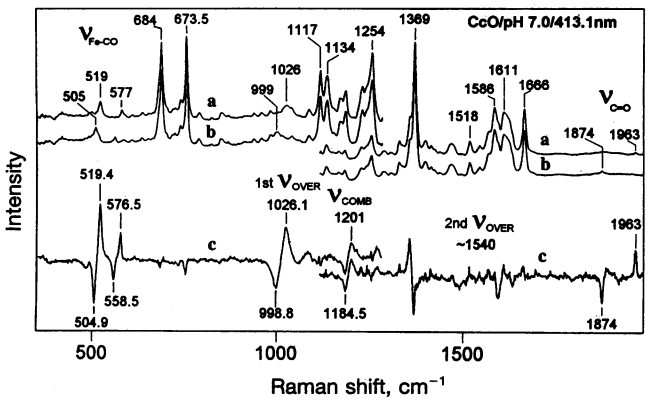

FIG. 1. Resonance Raman spectra of the $^{12}C^{16}O$-bound (spectrum a) and $^{13}C^{18}O$-bound (spectrum b) fully reduced cytochrome *c* oxidase (bovine heart) and the difference spectrum of spectrum a − spectrum b. The cytochrome *c* oxidase was solubilized in 100 mM sodium phosphate buffer/0.1% dodecyl β-D-maltoside, pH 7.0. The spectra were averaged for 20–30 min, with an excitation wavelength at 413.1 nm (≈1 mW). The isotope-sensitive lines at 519, 577, 1963 cm^{-1} are the ν_{Fe-CO}, δ_{Fe-CO}, and ν_{C-O}, respectively, and the lines at 1026 and 1201 cm^{-1} have been assigned as the overtone (ν_{over}) of ν_{Fe-CO} and the combination (ν_{comb}) between ν_{Fe-CO} and ν_7, respectively. The large apparent difference in the very strong ν_4 Raman line at 1368 cm^{-1} results from a slight difference in the degree of photodissociation of the two samples.

is coordinated by an imidazolate, such as in C*c*P (spectrum e), to the terminal oxidase family of proteins (spectra a–c) with a heme–Cu binuclear site (20). In general, the line in the 1000- to 1070-cm^{-1} region tends to be weaker than that in the 1180- to 1210-cm^{-1} region (I_{over}/I_{comb}, 0.8–1.0). However, for the terminal oxidase family of proteins this ratio is inverted (I_{over}/I_{comb}, 1.6–2.7).

To assign these new lines we compared the frequencies and the isotope shifts for all lines involving the CO (Table 1). For the line in the 1180- to 1210-cm^{-1} region the frequencies are within a few wavenumbers of the sum of ν_{Fe-CO} plus ν_7 (a symmetric porphyrin-stretching mode). In addition, the isotope shift is approximately the same as that of the fundamental mode. For the line in the 1000- to 1070-cm^{-1} region the frequency is slightly lower (5–15 cm^{-1}) than twice that of the ν_{Fe-CO} fundamental. Meanwhile, the isotope shifts for this line are all within a few wavenumbers of twice the isotope frequency shifts of the ν_{Fe-CO} fundamental. On the basis of these frequencies and isotope shifts we assign the line in the 1000- to 1070-cm^{-1} region as the overtone (ν_{over}) of the Fe–CO stretching mode and the line in the 1180- to 1210-cm^{-1} region as a combination (ν_{comb}) resulting from the sum of ν_{Fe-CO} and ν_7.

It is evident by inspection of Figs. 1 and 2 that the intensities of the overtone and combination lines are very high. Indeed, in the terminal oxidase family of proteins the integrated intensity of ν_{over} is even larger than that of the ν_{Fe-CO} fundamental. This high intensity of the Fe–CO overtone in heme proteins is surprising from an experimental point of view in that it was not detected previously. Although we have not systematically measured the intensity as a function of the incident laser excitation wavelength (Raman excitation profile), we have compared the intensity of the scattering in cytochrome bo_3 at two different wavelengths. With 413.1 nm (trace a of Fig. 2) the excitation is close to resonance with the 0–0 optical transition (a transition from $v = 0$ of the ground electronic state to $v = 0$ of the excited electronic state), where v is quantum number as illustrated schematically in Fig. 3, and the overtone scattering is very weak. However, by shifting the excitation to 406.7 nm ($\Delta\nu$ = ≈550 cm^{-1}), the incident wavelength is in approximate coincidence with a possible

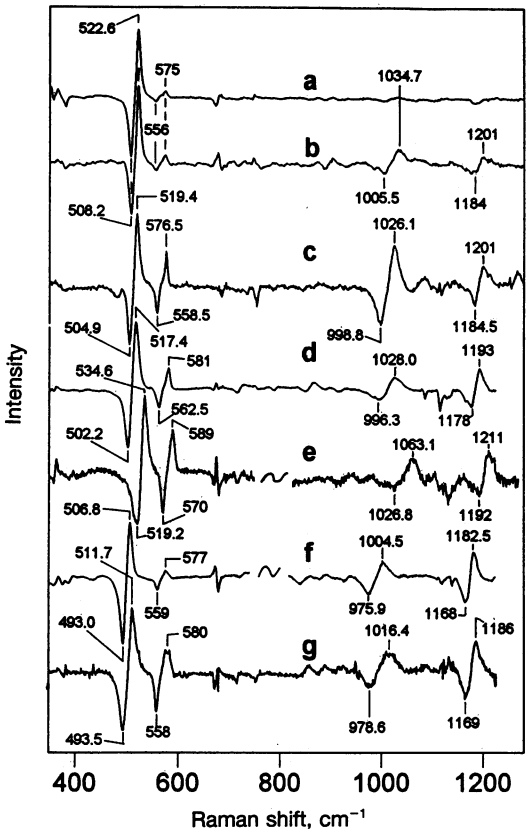

FIG. 2. Resonance Raman difference spectra of $^{12}C^{16}O$ adducts minus $^{13}C^{18}O$ adducts obtained from the *E. coli* quinol oxidase cytochrome bo_3 (spectra a and b); bovine cytochrome *c* oxidase (spectrum c); *Scapharca inaequivalvis* hemoglobin (spectrum d); yeast C*c*P (spectrum e); human adult hemoglobin (spectrum f); and horse skeletal myoglobin (spectrum g) at neutral pH. The spectra were averaged for 20–30 min at low-excitation laser power (0.1–1 mW). The excitation wavelength was 413.1 nm for all spectra except spectrum b, which was obtained with 406.7-nm excitation.

Fe–CO vibrational side band—i.e., the 0–1 excitation, and the intensity of ν_{over} (and ν_{comb}) is significantly enhanced (trace b in Fig. 2). For the other proteins examined the excitation was close to resonance with the 0–1 transition.

Enhancement Mechanisms. From a theoretical point of view the high intensity of the overtone is very surprising because quantitative calculations of the overtone intensity have predicted it to be very weak (21, 22). Thus, it is worthwhile to consider possible enhancement mechanisms.

When two modes have approximately the same frequency and have the same symmetry, Fermi resonance coupling may occur (23). The modes mix, shift apart in frequency, and share intensity. Consequently, when an isotopic substitution is made in an atom involved in one of the parent modes, the coupling is different. In that case both modes show isotopic sensitivity, the apparent isotope shifts are very different from theoretical expectations, and the intensity may be very different. The frequency shifts may even go in the opposite direction than that predicted for the isotope substitution. Anomalous isotopic frequency and intensity differences were not detected in the proteins we examined. Furthermore, some of the proteins have strong porphyrin modes in the regions of ν_{over} and ν_{comb} and others do not. On the basis of these observations enhancement of the overtone and combination by the Fermi resonance coupling to porphyrin modes is not a likely explanation of the data.

The Raman scattering intensity, in the usual description derived from second-order perturbation theory, is proportional to the square of the change in polarizability, which can

Table 1. Frequencies of the CO isotope-sensitive lines in several CO-bound heme proteins

Protein No.	Name	Soret max (Excitation)	δ_{Fe-C-O} (Isotope shift)	ν_{Fe-CO} (Isotope shift)	ν_{over} (Isotope shift)	$2\omega_e\chi_e$	ν_{comb} (Isotope shift)	$\nu_{Fe-CO} + \nu_7$ (ν_7)	I_{over}/I_{comb} (I_{over}/I_{Fe-CO})	ν_{Fe-His} (ref.)	ν_{C-O} (ref.)
1	Mb	424	580	511.7	1016.4	7.6	1186.0	1186.7	0.9	220 (14)	1944 (1)
		(413.1)	(22)	(18.2)	(37.8)		(17)	(675)	(0.5)		
2	HbA	419	577	506.8	1004.5	9.6	1182.5	1183.0	0.9	216 (14)	1952 (1)
		(413.1)	(18)	(13.8)	(28.6)		(14.5)	(676.2)	(0.3)		
3	HbI	420	581	517.4	1028.0	7.4	1193.0	1193.4	0.8	203 (14)	1945 (14)
		(413.1)	(19)	(15.2)	(31.7)		(15)	(676)	(0.3)		
4	CcP	423	589	534.6	1063.1	8.9	1211.0	1209.6	0.9	227/248 (16)	1923 (31)
		(413.1)	(19)	(15.4)	(36.3)		(19)	(675)	(0.4)		
5	HHO-2	420	573.7*	504.1*	997.6	9.7	1176.2	1179.1	1.0	215*	1963*
		(413.1)	(19)	(24.1)	(46.4)		(21.6)	(675)	(0.1)		
6	BH-aa_3	429	577	519.4	1026.1	11.8	1201.0	1202.4	2.7	214 (18)	1963 (12)
		(413.1)	(18)	(14.5)	(27.3)		(16.5)	(683)	(1.3)		
7	Rb-aa_3	430	574†	520.3†	1030.5	10.9	1199.8	1198.8	1.6	214 (19)	1966†
		(413.1)	(17)	(14.3)	(30.3)		(16.8)	(678.5)	(1.7)		
8	Para-aa_3	430	574‡	521.8‡	1030.3	11.3	1199.0	1200.5	2.5	Not measured	1967‡
		(413.1)	(19)	(16.8)	(29.8)		(16.0)	(683)	(0.9)		
9	Cyt-*bo*	416	575	522.6	1034.7	10.8	1201.0	1200.6	1.9	208 (15)	1960 (8)
		(406.7/413)	(19)	(14.4)	(29.2)		(17)	(678)	(0.5)		

All values are expressed in wavenumbers, except for the wavelength of the Soret maxima (max), which are expressed in nm. Values of the iron–histidine stretching mode (ν_{Fe-His}) are obtained from the five-coordinate form of the ferrous proteins. δ_{Fe-C-O}, ν_{Fe-CO}, and ν_{C-O} designate the Fe–C–O bending, Fe–CO stretching, and C–O stretching modes, respectively. ν_{over} and ν_{comb} refer to the overtone of ν_{Fe-CO} and the combination between ν_{Fe-CO} and ν_7. The anharmonicity ($2\omega_e\chi_e$) was estimated by $2\nu_{Fe-CO} - \nu_{over}$. The intensity ratio, I_{over}/I_{comb} (or I_{over}/I_{Fe-CO}), refers to the ratio of the intensity of ν_{over} to ν_{comb} (or ν_{over} to ν_{Fe-CO}). Isotope shifts are for the frequency obtained with $^{12}C^{16}O$–$^{13}C^{18}O$. Mb, horse skeletal myoglobin; HbA, human adult hemoglobin; HbI, *S. inaequivalvis* hemoglobin; HHO-2, the water-soluble fragment of isozyme 2 of the heme–heme oxygenase complex; BH-aa_3, cytochrome *c* oxidase from bovine heart; Rb-aa_3, *Rhodobacter sphaeroides* cytochrome *c* oxidase; Para-aa_3, cytochrome *c* oxidase from *Paracoccus denitrificans*; cyt-bo_3, quinol oxidase from *Escherichia coli*.

*S. T., M. Ikeda-Saito, and D.L.R., unpublished results.

†In addition to the lines at 520.3 cm^{-1} (ν_{Fe-CO}) and 1966 cm^{-1} (ν_{C-O}) assigned as from the α form, other lines at 493 cm^{-1} (ν_{Fe-CO}) and 1955 cm^{-1} (ν_{C-O}) were also identified (with equal intensity), which presumably results from the β form of the oxidases but shows almost no intensity of its overtone (17).

‡J.W., D.L.R., J. P. Hosler, and S. Ferguson-Miller, unpublished data.

be expressed by the sum of two leading terms, referred to as "A" and "B" (24). The A term, which involves linear coupling of harmonic potential energy surfaces (the Condon approximation), derives its intensity from Franck–Condon overlap factors between a slightly shifted or distorted excited electronic state and a ground electronic state. The B term (non-Condon) derives its intensity from vibronic mixing of two or more excited electronic states. In Raman measurements, when the incident laser is in resonance with strong electronic transitions, such as the Soret band in heme proteins, A-term scattering is the dominant scattering mechanism, whereas when it is in resonance with weak transitions, such as the visible-region Q-band in heme proteins, B-term scattering is dominant through mixing between this weak transition and the strong Soret transition.

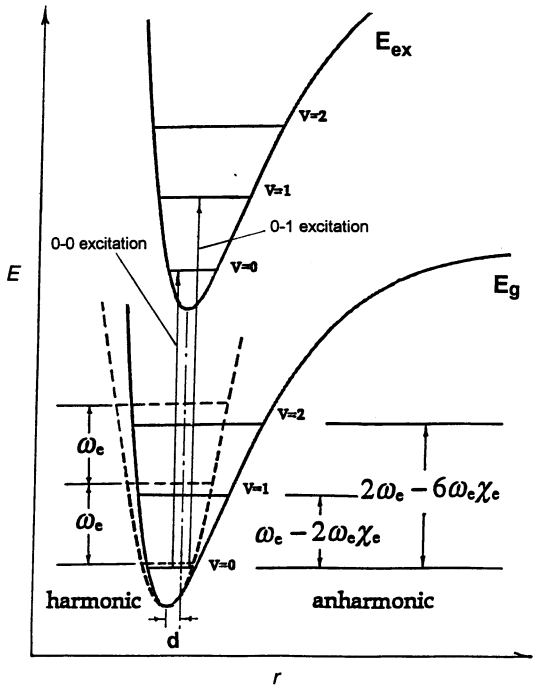

FIG. 3. Schematic diagram of the nuclear coordinate dependence, *r*, of the molecular potentials for a diatomic oscillator. Comparison between a harmonic (- - -) and an anharmonic potential (—) is illustrated along with the relevant anharmonicity parameters used in the text. Ground (E_g) and excited (E_{ex}) state potentials are displaced by an amount *d*.

Over the past several years Champion and coworkers (25) have developed a quantitative description of the scattering processes with a transform theory in which electron–nuclear coupling strengths (*S*), which are proportional to the ratio of the overtone intensity to that of the fundamental, are derived from absolute Raman scattering cross sections. The coupling strengths are generally small for the porphyrin modes because the electronic transitions are distributed over many nuclei. A study of the fundamental Fe–CO stretching mode in MbCO yielded only a Condon (A term) coupling strength of 0.027, predicting that the intensity of the overtone should be ≈3% of that of the fundamental. However, in our experiment on MbCO we find that the intensity of the Fe–CO stretching-mode overtone is ≈50% of the fundamental, more than one order of magnitude greater than that predicted from the transform theory.

It has been reported that certain symmetric heme modes have large non-Condon (B term) contributions, even when excited in the Soret transition (21), and several other theoretical treatments have also identified the importance of non-Condon effects (26, 27). Using simple overlap-factor calcula-

tions, we found that by adding in a significant degree of non-Condon scattering, we could increase the relative intensity of the overtone to be consistent with the data. However, when Champion and coworkers incorporated non-Condon scattering into the amplitude for the excitation profile of the fundamental ν_{Fe-CO} mode in Mb–CO with the transform theory, they were unable to fit the data (13). The application of other theoretical treatments of the ν_{Fe-CO} mode, including higher-order effects, have not been reported, and thus none of the conventional bound-state resonance Raman theories can account for our results at present.

The vibrational properties of the Fe–CO bond may be perturbed by involvement of dissociative electronic states. Excitation into the Soret transition of CO-bound heme proteins leads to Fe–CO bond cleavage due to a mixing or strong coupling between the porphyrin π–π^* transition and either d–d or charge-transfer transitions involving the Fe–CO linkage. Porphyrin (π) to iron (d_{z^2}) and iron (d_π) to CO (π^*) charge-transfer transitions and d_{xy} to $d_{x^2-y^2}$ ligand field transitions have all been proposed to fall in the near-UV region (28, 29). These optical transitions may be too weak to be detected in the absorption spectrum but may play an important role in the Raman scattering and in the photolysis of CO from the proteins. The mixing between the porphyrin π transitions and these dissociative states results in a level of complexity that should be included in Raman theories. Our findings clearly call for a careful re-examination of the scattering theory for heme-associated modes, such as ν_{Fe-CO}, which lie on a dissociative potential surface.

Structure Correlations. In a simple diatomic model approximation, molecular potentials with a progressive set of vibrational levels, such as those depicted in Fig. 3, are obtained. The separation between the levels steadily decreases toward the dissociation limit. This decrease in spacing is the anharmonicity of the potential function and reflects the dissociation energy of the oscillator: the greater the anharmonicity, the more rapidly the levels become closer together and the smaller the dissociation energy. Also, due to the anharmonicity the average of the internuclear distance of the oscillator increases in comparison to that of the equilibrium internuclear distance in the ground state as one progresses toward the dissociation limit. The higher levels serve as a probe of the environment further away from the equilibrium distance. In the case of the Fe–CO stretching mode in heme proteins, the anharmonicity can be sensitive to the distal environment.

The energy levels, ε_v, for an anharmonic potential may be written (30) to lowest order as follows:

$$\varepsilon_v = \omega_e(v + 1/2) - \omega_e\chi_e(v + 1/2)^2. \quad [1]$$

The constant, ω_e, is the spacing between the adjacent energy levels with quantum number, v, for a harmonic potential, and $\omega_e\chi_e$ is referred to as the anharmonicity factor. The difference between the frequency of the first overtone (0–2 transition) and twice the frequency of fundamental (0–1 transition) is given by $2\omega_e\chi_e$. In Table 1 the values of $2\omega_e\chi_e$ range from 7 to 12 cm^{-1}. From the data in this Table it is evident that there is no correlation between anharmonicity and Fe–CO stretching frequency. Similarly, there is no correlation between Fe–CO stretching frequency and ratio of intensity of overtone-to-combination mode.

The properties of the proximal ligand can affect bonding between the iron and the distal ligand and, thus, its vibrational frequencies (1). The frequency of the iron–histidine stretching mode (ν_{Fe-His}) is a measure of the bond strength between the iron atom and the histidine. Table 1 shows that despite a variation in the frequency of ν_{Fe-His} from 203 cm^{-1} for *S. inaequivalis* hemoglobin to 227/248 cm^{-1} for the imidazolate-coordinate C*c*P, the anharmonicities of all of the proteins other than the oxidases lie between 7.4 and 9.6 cm^{-1}, and the overtone/combination intensity ratios lie in the 0.8–1.0 range. The ν_{Fe-His} values from proteins in the oxidase family are in the middle of the frequency distribution, ranging from 209 to 214 cm^{-1}, but the anharmonicity values (10.8–11.8) and the overtone-to-combination intensity ratio (1.6–2.7) for the terminal oxidases are all higher than those of any of the other proteins. We conclude that neither the charge (imidazole or imidazolate) of the proximal histidine nor the strength of the iron–histidine bond correlates with the behavior of the higher-order modes involving the CO.

We have also examined the relationship (Fig. 4) between the C–O stretching mode and anharmonicity and found that, except for the C*c*P point, these variables clearly correlate. CO coordinates to the heme-iron atom (*i*) through a σ bond formed by the lone pair on the CO and the iron d_{z^2} orbital and (*ii*) through π-backbonding from the iron d_π orbital to the π^* orbital of the CO (1). The reduction of the C–O stretching frequency from $\approx$2145 cm^{-1} in the free gas to $\approx$1950 cm^{-1} in heme proteins is a consequence of this back donation. An increase in the d_π–π^* overlap increases the Fe–CO bond order and concomitantly decreases the C–O bond order due to the population of the antibonding π orbitals on the CO. Thus, any electronic interaction that affects the π bonding will affect the Fe–CO and the C–O bond strengths, accounting for the well established inverse correlation between the stretching frequencies of these bonds (1). However, because the frequency of ν_{C-O} is high and the mode is isolated from other modes, it is less susceptible to vibrational coupling and geometric changes than ν_{Fe-CO} and, thus, is a more reliable marker of the iron d_π to the CO π^* backbonding than is ν_{Fe-CO}.

From the above considerations the correlation in Fig. 4 can be understood. The C–O stretching frequency is a marker of the back donation to the CO π^* orbital. Thus, ν_{C-O} should correlate with the d_π–π^* overlap contribution to the Fe–CO binding energy, which is reflected in the anharmonicity of the Fe–CO stretching mode more sensitively than in the frequency of the fundamental Fe–CO mode. For a simple Morse potential the anharmonicity is inversely proportional to the dissociation energy (30). Thus, the larger the anharmonicity, the lower the dissociation energy and the weaker the Fe–CO bond. Therefore, the CO-binding energy would be expected to vary inversely with both anharmonicity of the Fe–CO potential and the C–O stretching frequency. The failure of C*c*P to lie on the correlation curve most likely results from the hydrogen bond to the bound CO in this protein (31), an interaction that is not

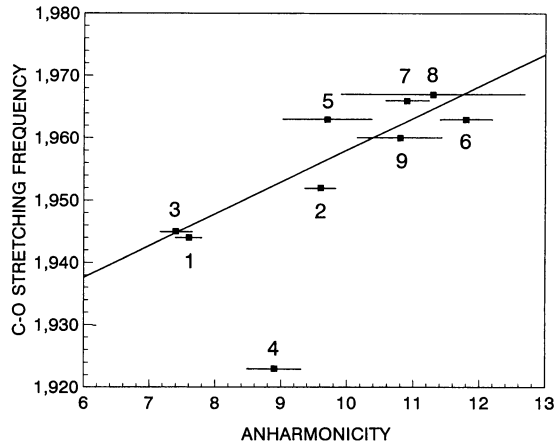

FIG. 4. Anharmonicity ($2\omega_e\chi_e$) data (in cm^{-1}) from the proteins listed in Table 1 is plotted vs. their ν_{C-O} frequencies (cm^{-1}). Error bars were the result of several measurements of the anharmonicity and vary depending on the signal-to-noise in the spectra, whereas the error in the C–O stretching frequency for all points is about ± 1 cm^{-1}. The line is a least-squares fit to the data for all points except point 4 (C*c*P), which lies off the correlation, as discussed in text.

thought to be present in any of the other proteins we have examined, although an effect due to the imidazolate rather than imidazole coordination on the proximal side of the heme in C*c*P cannot be excluded.

The terminal oxidase family of enzymes do not lie on the well-established inverse correlation curve between ν_{Fe-CO} and ν_{C-O} in histidine-coordinated heme proteins (32). This relationship has recently been attributed to a geometry change of the Fe–C bond due to a steric interaction between the bound CO and the Cu atom (17), which is known to be located 3–5 Å from the heme-iron atom (20). Interestingly, despite this geometry change in the terminal oxidases, they still fall on the anharmonicity vs. ν_{C-O} correlation curve, which indicates that the alteration of the Fe–CO geometry caused by the steric constraint of the nearby copper atom does not perturb the shape of the Fe–C bond energy potential. In addition, the behavior of the terminal oxidases is distinct from that of C*c*P, in which hydrogen bonding to the bound CO or the imidazolate coordination modifies its electronic structure such that it fails to lie on the anharmonicity vs. ν_{C-O} correlation curve. These contrasting results illustrate the necessity to obtain frequency and anharmonicity data for a complete understanding of heme protein–ligand energetics.

We are indebted to Dr. P. Champion of Northeastern University and John Shelnutt of Sandia National Laboratories for several stimulating discussions. We thank Dr. A. Boffi of the University of Rome for *S. inaequivalvis* hemoglobin and human adult hemoglobin, Drs. S. Ferguson-Miller and J. P. Hosler of Michigan State University for cytochromes aa_3 from *R. sphaeroides* and *P. denitrificans*, and Dr. M. Ikeda-Saito of Case Western Reserve University for the heme–heme oxygenase complex. This work was supported by National Institutes of Health Grant GM48714 to D.L.R.

1. Yu, N.-T. & Kerr, E. A. (1988) in *Biological Applications of Raman Spectroscopy*, ed. Spiro, T. G. (Wiley, New York), pp. 39–95.
2. Ray, G. B., Li, X.-Y., Ibers, J. A., Sesseler, J. L. & Spiro, T. G. (1994) *J. Am. Chem. Soc.* **116,** 162–176.
3. Frauenfelder, H., Sligar, S. G. & Wolynes, P. G. (1991) *Science* **254,** 1598–1603.
4. Parak, F. & Frauenfelder, H. (1993) *Physica A* **201,** 332–345.
5. Wang, J., Takahashi, S. & Rousseau, D. L. (1994) in *Proceedings of the 14th International Conference on Raman Spectroscopy*, eds. Yu, N.-T. & Li, X.-Y. (Wiley, New York), pp. 118–119.
6. Hirota, S., Ogura, T., Appelman, E. H., Shinzawa-Itoh, K., Yoshikawa, S. & Kitagawa, T. (1994) *J. Am. Chem. Soc.* **116,** 10564–10570.
7. Yonetani, T. (1960) *J. Biol. Chem.* **235,** 845–852.
8. Hill, J. J., Goswitz, V. C., Calhoun, M., Carcia-Horsman, J. A., Lemieux, L., Alben, J. O. & Gennis, R. B. (1992) *Biochemistry* **31,** 11435–11440.
9. Wang, J., Boldt, N. J. & Ondrias, M. R. (1992) *Biochemistry* **31,** 867–878.
10. Wang, J., Rousseau, D. L., Abu-Soud, H. M. & Stuehr, D. J. (1994) *Proc. Natl. Acad. Sci. USA* **91,** 10512–10516.
11. Argade, P. V., Ching, Y.-C. & Rousseau, D. L. (1984) *Science* **255,** 329–331.
12. Yoshikawa, S., Choc, M. G., O'Toole, M. C. & Caughey, W. S. (1977) *J. Biol. Chem.* **252,** 5498–5508.
13. Gu, Y. (1994) Ph.D. dissertation (Northeastern University, Boston).
14. Song, S., Boffi, A., Chiancone, E. & Rousseau, D. L. (1993) *Biochemistry* **32,** 6330–6336.
15. Tsubaki, M., Mogi, T., Hori, H., Hirota, S., Ogura, T., Kitagawa, T. & Anraku, Y. (1994) *J. Biol. Chem.* **269,** 30861–30868.
16. Hashimoto, S., Teraoka, J., Inubishi, T., Yonetani, T. & Kitagawa, T. (1986) *J. Biol. Chem.* **261,** 11110–11118.
17. Wang, J., Takahashi, S., Hosler, J. P., Mitchell, D. M., Ferguson-Miller, S., Gennis, R. B. & Rousseau, D. L. (1995) *Biochemistry* **34,** 9818–9825.
18. Salmeen, I., Rimai, L. & Babcock, G. T. (1978) *Biochemistry* **17,** 800–806.
19. Hosler, J. P., Fetter, J., Tecklenburg, M. M. J., Espe, M., Lerma, C. & Ferguson-Miller, S. (1992) *J. Biol. Chem.* **267,** 24264–24272.
20. Tsukihara, T., Aoyama, H., Yamashita, E., Tomizaki, T., Yamaguchi, H., Shinzawa-Itoh, K., Nakajima, R., Yaono, R. & Yoshikawa, S. (1995) *Science*, in press.
21. Morikis, D., Li, P., Bangcharoenpaurpong, O., Sage, J. T. & Champion, P. M. (1991) *J. Phys. Chem.* **95,** 3391–3398.
22. Stallard, B. R., Champion, P. M., Callis, P. R. & Albrecht, A. C. (1983) *J. Chem. Phys.* **78,** 712–722.
23. Proniewicz, L. M. & Kincaid, J. R. (1990) *J. Am. Chem. Soc.* **112,** 675–681.
24. Tang, J. & Albrecht, A. C. (1970) in *Raman Spectroscopy*, ed. Szmanski, H. (Plenum, New York), Vol. 2, pp. 33–68.
25. Gu, Y. & Champion, P. M. (1990) *Chem. Phys. Lett.* **171,** 254–258.
26. Shelnutt, J. A. (1980) *J. Chem. Phys.* **72,** 3948–3958.
27. Zgierski, M. Z. (1987) *Chem. Phys. Lett.* **136,** 252–257.
28. Makinen, M. W. & Churg, A. K. (1983) in *Iron Porphyrins: Part One*, eds. Lever, A. B. P. & Gray, H. B. (Addison–Wesley, Reading, MA), pp. 141–235.
29. Eaton, W. A. & Hofrichter, J. (1981) *Methods Enzymol.* **76,** 175–261.
30. Herzberg, G. (1950) *Molecular Spectra and Structure* (Van Nostrand Reinhold, New York).
31. Satterlee, J. D. & Erman, J. E. (1984) *J. Am. Chem. Soc.* **106,** 1139–1140.
32. Rousseau, D. L., Ching, Y.-C. & Wang, J. (1993) *J. Bioenerg. Biomembr.* **25,** 165–176.